



# EXCITATION OF THE STONELEY–SCHOLTE WAVE AT THE BOUNDARY BETWEEN AN IDEAL FLUID AND A VISCOELASTIC SOLID

N. FAVRETTO-ANRÈS AND G. RABAU

*Centre National de la Recherche Scientifique, Laboratoire de Mécanique et d'Acoustique,  
Équipe Acoustique Sous-Marine et Modélisation, 31 chemin Joseph Aiguier,  
13402 Marseille CEDEX 20, France*

*(Received 8 May 1996, and in final form 11 November 1996)*

The predicted properties of the Stoneley–Scholte wave, deduced from a previous theoretical study, are experimentally verified at the boundary between an ideal fluid and a viscoelastic solid, respectively represented by water and synthetic resins (PVC and B2900). In particular, it is quantitatively shown that the damping of the energy of the interface wave increases with the distance from the interface and with the distance of propagation. The method of generation of the Stoneley–Scholte wave is based on the association of a shear wave transducer with a solid wedge. The method, previously developed for the ideal fluid/elastic solid interface, is here adapted for the boundary between water and a viscoelastic solid.

© 1997 Academic Press Limited

## 1. INTRODUCTION

For many years, the analysis of surface or interface waves has been widely developed. In particular, the Stoneley–Scholte wave, also called the Scholte wave, has been studied both theoretically and experimentally [1, Poirée and Luppé 1991]. The wave propagates at the boundary between a fluid and a solid, and it has proved to be a useful tool in non-destructive testing (NDT) or in marine seismology for the acoustical characterization of the first layer of the sea floor [2, Jensen and Schmidt 1986]. In particular, since the velocity of the Stoneley–Scholte wave is strongly linked to the shear wave velocity of the sedimentary bottom, one can easily obtain accurate information about the shear wave velocity of the sediments by applying inversion techniques to the dispersion curves of the interface wave [3, Caiti *et al.* 1991]. On the contrary, coring, sampling or direct *in situ* techniques may significantly affect the values of the shear wave velocity of the sediment samples. To obtain information about the shear wave attenuation of the sediments from the propagation characteristics of the Stoneley–Scholte wave, one has to take into account the dissipative property of the solid in the theoretical models of the propagation of the interface wave. The structure of the Stoneley–Scholte wave is usually analyzed at the boundary between a viscous fluid and an elastic solid [4, Vol'kenshtein and Levin 1988]. However, very few studies have dealt with an attenuating solid.

The first author has previously conducted a theoretical study of the propagation of the Stoneley–Scholte wave at the plane boundary between in ideal fluid and a viscoelastic solid, which models the water/sediments interface [5, Favretto-Anrès 1996]. The solid was represented by a Kelvin–Voigt solid. The viscosity coefficients introduced in the constitutive law were then connected to the attenuations of the homogeneous plane waves

in the solid, which can easily be determined by acoustical measurements. The analysis of the Stoneley–Scholte wave was developed by using the approach of inhomogeneous plane waves. It enabled one to describe the interface wave locally as a linear combination of three inhomogeneous plane waves, satisfying boundary conditions at the interface in each medium. It was shown that the energy is concentrated in the solid material and that it decreases with the distance from the interface. The originality of the study was to quantify the damping of the Stoneley–Scholte wave at the interface during its propagation. Some of these characteristics are reviewed in sections 1 and 2. Herein the experimental confirmation of these properties is reported, and in particular the confirmation of the damping of the interface wave during its propagation at the boundary between water and viscoelastic solids. This property has not been explicitly verified in other works. There is no way of exciting a Stoneley–Scholte wave at the water/solid interface by means of a plane incident wave in the water, because its speed is always less than the speed of sound in the fluid. Many scientists have proposed experimental methods for generating this interface wave: the liquid-wedge method [6, Luppé and Doucet 1988], the method based on the conversion of a Rayleigh wave into a Stoneley–Scholte wave on a surface partially immersed in a liquid [7, de Billy and Quentin 1983], the method based on mode conversion on a periodically rough surface [8, Claeys *et al.* 1983], the method using interdigitated transducers [9, Guzhev *et al.* 1984], etc. The method chosen here is the solid wedge method, used for generating a Rayleigh wave at the free surface of a solid [10, Viktorov 1967]. The wedge was associated with a shear wave transducer. The method, previously developed at the water/elastic solid interface [11, Guilbot 1994], is based on the mode conversion of an incident shear wave in the solid wedge into an interface wave at the critical angle. The experiments, carried out at the boundary between water and synthetic resins (PVC and B2900), are described in section 3. The originality of the experimental study is that it involves an attenuating solid medium. The experimental results demonstrate the validity of the theoretical model developed for the ideal fluid/viscoelastic solid interface.

## 2. REVIEW OF SOME PROPERTIES OF INHOMOGENEOUS PLANE WAVES

The propagation of inhomogeneous plane waves in fluid and solid media has been studied in previous papers [12, Poirée 1989; 13, Poirée 1991; 14, Deschamps 1991; 4, Favretto-Anrès 1996]. A synthetic summary is presented in this section.

### 2.1. IN A VISCOELASTIC SOLID MEDIUM

Two inhomogeneous (heterogeneous) plane waves can propagate into a solid medium, supposed to be viscoelastic, homogeneous, isotropic and infinite: a lamellar one ( $\mathbf{rot} \boldsymbol{\zeta}_L = \mathbf{0}$ ) and a torsional one ( $\mathbf{div} \boldsymbol{\zeta}_T = 0$ ). The acoustic real valued displacements  $\zeta_L$  and  $\zeta_T$  associated with these waves have the general form:

$$\zeta_M = \text{Re}[\zeta_M^*], \quad (1)$$

with

$$\zeta_M^* = \zeta_M^{*0} \exp(i\mathbf{K}_M^* \cdot \mathbf{r}), \quad \mathbf{K}_M^* = \mathbf{K}'_M + i\mathbf{K}''_M, \quad \mathbf{K}_M^* \cdot \mathbf{K}_M^* = k_m^2(1 + i\omega v_m). \quad (2-4)$$

The subscript  $M = L, T$  is used to denote the lamellar and torsional waves.  $\zeta_M^{*0}$  is a complex valued constant vector and  $\mathbf{K}_M^*$  is the complex-valued wave vector of the inhomogeneous waves. The real valued vectors  $\mathbf{K}'_M$  and  $\mathbf{K}''_M$ , respectively, represent the propagation and the attenuation of the wave.  $k_m$  are the wavenumbers of the associated homogeneous plane waves (longitudinal ( $m \sim l$ ) and shear ( $m \sim t$ ) ones). The quantities  $v_{(m \sim l)}(\omega) = (2M' + A')/\rho c_l^2$  and  $v_{(m \sim t)}(\omega) = M'/\rho c_t^2$  define the ratio between the viscosity

and the Lamé coefficients,  $\rho$  being the density of the solid and  $c_m$  the velocity of the homogeneous plane waves.  $\mathbf{r}$  is the space vector and  $\omega$  is the angular frequency.

## 2.2. IN AN IDEAL FLUID MEDIUM

Only one inhomogeneous (evanescent) plane wave can propagate into an ideal fluid: a lamellar one (*rot*  $\zeta_F = \mathbf{0}$ ). The real valued displacement  $\zeta_F$  in the fluid is described, from the complex valued displacement  $\zeta_F^*$ , by the equations

$$\zeta_F = \text{Re}[\zeta_F^*], \quad \zeta_F^* = \zeta_F^{*0} \exp(i\mathbf{K}_F^* \cdot \mathbf{r}), \quad (5, 6)$$

$$\mathbf{K}_F^* = \mathbf{K}'_F + i\mathbf{K}''_F, \quad \mathbf{K}_F^* \cdot \mathbf{K}_F^* = k_0^2. \quad (7, 8)$$

The term  $\zeta_F^{*0}$  is a complex valued constant vector,  $\mathbf{K}_F^*$  is the complex valued wave vector of the lamellar wave,  $k_0 = \omega/c_0$  is the wavenumber of the associated homogeneous wave,  $c_0 = A_0/\rho_0$  is the longitudinal wave velocity,  $\rho_0$  is the fluid density and  $A_0$  is the Lamé coefficient.

## 3. THE STONELEY–SCHOLTE WAVE AT THE PLANE BOUNDARY BETWEEN AN IDEAL FLUID AND A VISCOELASTIC SOLID: SOME THEORETICAL RESULTS

Recently, the propagation of the Stoneley–Scholte wave has been theoretically analyzed at the plane boundary between an ideal fluid and a viscoelastic solid [4, Favretto-Anrès 1996]. The two media were supposed to be homogeneous, isotropic and semi-infinite. The interface wave was locally represented in the form of a linear combination of three inhomogeneous waves (one evanescent wave in the fluid and two heterogeneous waves in the solid).

### 3.1. THE EQUATION OF DISPERSION

One now introduces the perpendicular axes  $Ox_1$  and  $Ox_2$  with unit vectors  $\mathbf{x}_1$  and  $\mathbf{x}_2$  such that the interface lies along  $Ox_1$ , the fluid medium being defined by  $x_2 > 0$  and the solid one by  $x_2 < 0$ .

The displacement of the lamellar evanescent wave in the fluid and those of the lamellar and torsional heterogeneous waves in the viscoelastic solid are described in section 2. All of these waves have the same projection  $\mathbf{K}_1^*$  of their wave vectors upon the axis  $\mathbf{x}_1$ . After having written the required conditions of continuity at the interface ( $x_2 = 0$ ), one finds that the characteristic equation of the Stoneley–Scholte wave in the unknown  $K_1^*$  is

$$(K_1^{*2} - K_{T_2}^{*2})W + 2K_1^{*2}K_{L_2}^*K_{T_2}^*X = (\rho_0/\rho)(K_{L_2}^*/K_{T_2}^*)k_t^4(1 - i\omega v_t), \quad (9)$$

with

$$K_{L_2}^* = \pm(k_t^2(1 + i\omega v_t) - K_1^{*2}), \quad K_{T_2}^* = \pm(k_t^2(1 + i\omega v_t) - K_1^{*2}), \quad K_{P_2}^* = \pm(k_0^2 - K_1^{*2}), \quad (10-12)$$

$$W = 2K_1^{*2}(1 - i\omega v_\theta) + i\omega(c_t^2/c_t^2)(v_t K_{L_2}^{*2} + v_\theta K_1^{*2}) - Y, \quad (13)$$

$$Y = k_t^2(1 + i\omega v_t), \quad X = 2(1 - i\omega v_\theta) + i\omega(c_t^2/c_t^2)(v_\theta - v_t), \quad (14, 15)$$

$$v_\theta = (c_t^2 v_t - 2c_t^2 v_t)/(c_t^2 - 2c_t^2). \quad (16)$$

The terms  $K_{M1}$  and  $K_{M2}$  are the projections of the vector  $\mathbf{K}_M$  upon the axes  $\mathbf{x}_1$  and  $\mathbf{x}_2$ . The quantity  $\alpha_l$  (respectively,  $\alpha_t$ ) defines the attenuation of the longitudinal (respectively, shear) plane wave in the solid medium.

The solution of equation (9) in the complex plane  $K_1^*$  gives the Stoneley–Scholte wave velocity and attenuation for a given frequency. The different wave vectors satisfy the inequalities

$$\text{Im}(K_{L2}^*, K_{T2}^*) < 0, \quad \text{Im}(K_S^*) > 0, \quad (17, 18)$$

which express the finite energy condition in both media.

The densities of the energy in the fluid  $W_F$  and in the solid  $W_S$ , associated with the Stoneley–Scholte wave, are expressed in terms of the components of the strain tensor  $\mathbf{E}$ , and implicitly in terms of the displacements as follows:

$$W_F(\omega) = \frac{1}{2}\rho_0 c_0^2 \text{Re}(\mathbf{E}_{ii} \bar{\mathbf{E}}_{ii}), \quad (19)$$

with

$$E_{11}(\omega) = i \frac{K_1^{*2} + K_{T2}^{*2}}{2K_{L2}^*} \exp(iK_{L2}^* x_2) V, \quad E_{22}(\omega) = iK_{L2}^* \frac{K_1^{*2} + K_{T2}^{*2}}{2K_1^{*2}} \exp(iK_{L2}^* x_2) V, \quad (20)$$

$$\begin{aligned} W_S(\omega) = & \rho c_t^2 \sum_{i,j=1,2} \text{Re}[(1 - i\omega v_t) E_{ij} \bar{\mathbf{E}}_{ij}] \\ & + \frac{1}{2}\rho(c_t^2 - 2c_l^2) \text{Re} \left[ (1 - i\omega v_\theta) \sum_{i=1,2} E_{ii} \sum_{i=1,2} \bar{\mathbf{E}}_{ii} \right], \end{aligned} \quad (21)$$

with

$$\begin{aligned} E_{11}(\omega) = & -i \left\{ \frac{K_1^{*2} - K_{T2}^{*2}}{2K_{L2}^*} \exp(iK_{L2}^* x_2) + K_{T2}^* \exp(iK_{T2}^* x_2) \right\} V, \\ E_{22}(\omega) = & -i \left\{ K_{L2}^* \frac{K_1^{*2} - K_{T2}^{*2}}{2K_1^{*2}} \exp(iK_{L2}^* x_2) - K_{T2}^* \exp(iK_{T2}^* x_2) \right\} V, \\ E_{12}(\omega) = & -i \frac{K_1^{*2} - K_{T2}^{*2}}{2K_1^*} \left\{ \exp(iK_{L2}^* x_2) - \exp(iK_{T2}^* x_2) \right\} V, \quad V = \exp(iK_1^* x_1). \end{aligned} \quad (22)$$

$\bar{\mathbf{E}}_{ij}$  is the complex-conjugate of  $E_{ij}$ . The density of the energy in each medium thus decreases exponentially from both sides of the interface. Damped propagation takes place along the interface with a speed  $c_{sch}$ :

$$c_{sch} = \omega/K_1', \quad K_1' = \text{Re}(K_1^*) > \max(k_0, k_t, k_l). \quad (23)$$

### 3.3. NUMERICAL APPLICATIONS: THE WATER/B2900 AND THE WATER/PVC INTERFACES

The ideal fluid was represented by water. The viscoelastic solid was represented by B2900, a synthetic resin loaded with alumina and tungsten ( $c_l > c_t > c_0$ ) and then by PVC ( $c_t < c_0 < c_l$ ). The acoustical characteristics of the media, assumed constant in the frequency range 10 kHz–1 MHz, are summarized in Table 1. The attenuations of the homogeneous plane waves in the solid increase with frequency (see Figures 1 and 2). For 500 kHz, the longitudinal wave attenuations were 110 dB/m for B2900 and 130 dB/m for PVC, and the shear wave attenuations were 180 dB/m for B2900 and 490 dB/m for PVC.

TABLE 1

*Some measured characteristics of the fluid (water) and the solids (B2900 and PVC)*

Frequencies 10 kHz–1 MHz	Density (kg/m <sup>3</sup> )	LW velocity (m/s)	SW velocity (m/s)
Water	1000	1478	—
PVC	1360	2270	1100
B2900	2000	2910	1620

The numerical solution of equation (9), for example for 60 kHz, provided the results in Table 2. The dispersion curves of the phase and group velocities of the Stoneley–Scholte wave (see Figure 3) show that the dispersion is weak and that it takes place in only a small frequency range (10–60 kHz). The instability of the group speed values is due to the experimental attenuation of the homogeneous plane waves which was taken into account to calculate the velocities. Indeed, the attenuations can be accurately obtained only for every second kilohertz, in frequency range used. The distribution of the acoustical energy in both media (fluid and solid) as a function of the distance from the interface shows that energy is concentrated in the solid and does not penetrate deep into the two media (see Figure 4). However, above all, the energy of the interface wave is quickly attenuated during its propagation at the boundary between water and the viscoelastic solids (see Figure 5). These remarks reveal the difficulty in detecting the Stoneley–Scholte wave at the water/viscoelastic solid interface.

#### 4. THE STONELEY–SCHOLTE WAVE AT THE PLANE BOUNDARY BETWEEN AN IDEAL FLUID AND A VISCOELASTIC SOLID: SOME EXPERIMENTAL RESULTS

Two kinds of experiments were carried out. In the first, the ideal fluid was represented by water and the viscoelastic solid by PVC material; in the second, the viscoelastic solid was represented by a synthetic resin called B2900. The purpose was to verify experimentally, the properties deduced from the theoretical study of Stoneley–Scholte wave propagation, at the boundary between water and viscoelastic solids, such as the phase velocity of the wave and the dependence of the energy damping on the distance from the

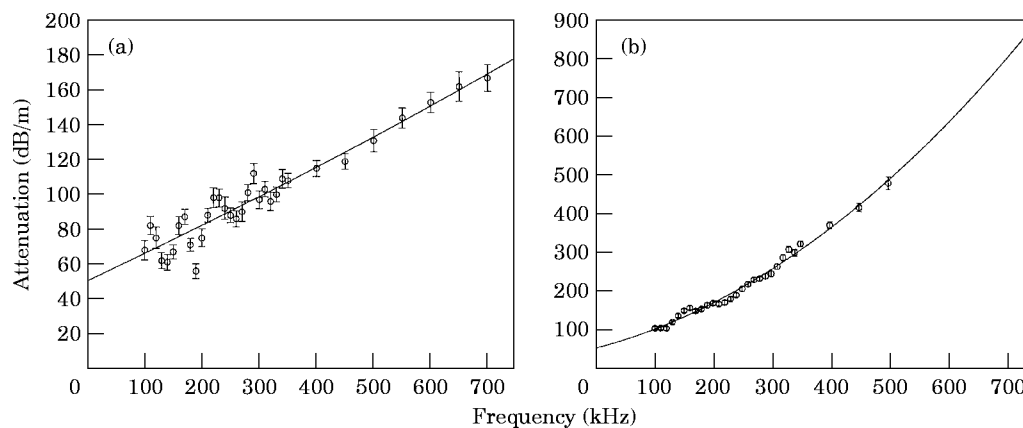


Figure 1. Measured attenuations of the homogeneous plane waves in PVC material. (a) Longitudinal waves; (b) shear waves.  $\circ$ , Experimental values; I, error ranges.

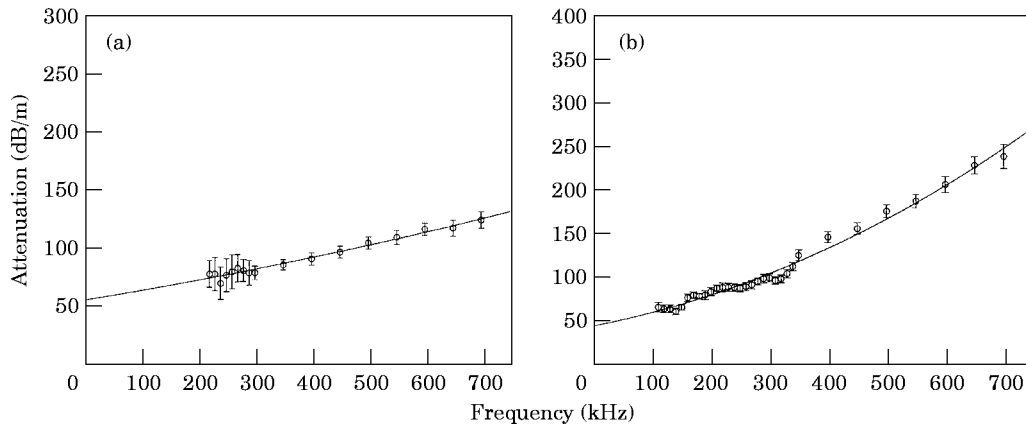


Figure 2. Measured attenuations of the homogeneous plane waves in B2900 material. (a) Longitudinal waves; (b) shear waves.  $\circ$ , Experimental values; I, error ranges.

TABLE 2

*Theoretical results about the projection of the different wave vectors upon the axes and the velocity of the interface wave (frequency 60 kHz)*

Frequency 60 kHz	$K_2^*$ ( $\text{m}^{-1}$ )	$K_2^*$ ( $\text{m}^{-1}$ )	$K_2^*$ ( $\text{m}^{-1}$ )	$K_1^*$ ( $\text{m}^{-1}$ )	$c_{sch}$ (m/s)
PVC	9-391i	7-251i	-14 + 340i	425 + 11i	887
B2900	4-268i	3-186i	-13 + 154i	298 + 7i	1266

interface. In particular, it was desired to determine quantitatively the damping of the energy of the interface wave in function of propagation distance.

#### 4.1. DESCRIPTION OF THE EXPERIMENTAL SET-UP

A schematic representation of the principles of the experiments is shown in Figure 6. The Stoneley-Scholte wave was generated by a solid wedge excited by a shear wave

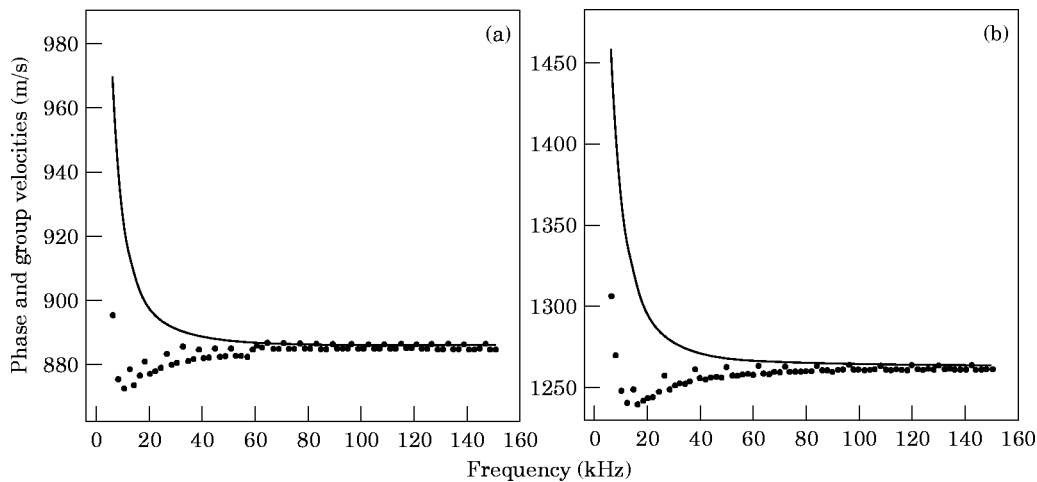


Figure 3. Theoretical dispersion curves of the phase (—) and group ( $\cdots$ ) velocities of the Stoneley-Scholte wave. (a) For the water/PVC interface; (b) for the water/B2900 interface.

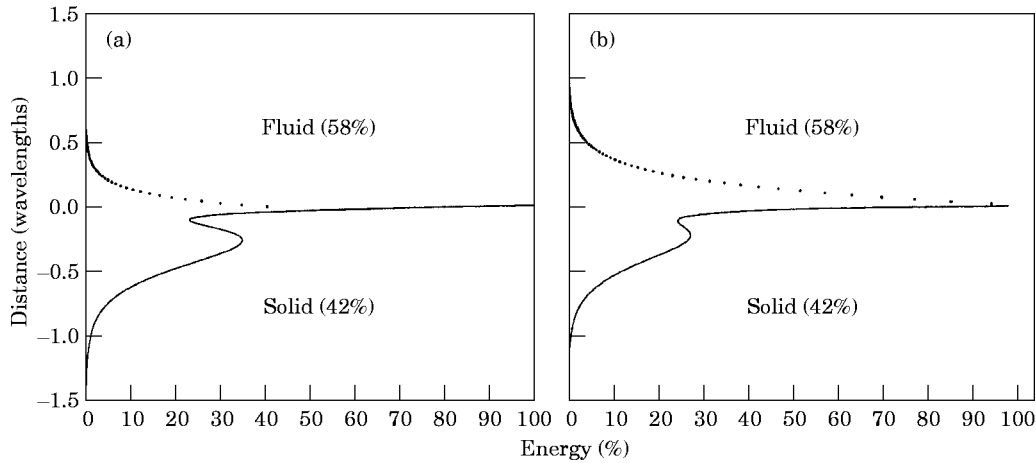


Figure 4. The theoretical distribution of the acoustical energy as a function of distance from the interface. (a) Water/PVC; (b) water/B2900. Frequency 60 kHz, wavelengths  $\lambda = 2.1$  cm for B2900 and  $\lambda = 1.5$  cm for PVC, distance of propagation 20 cm; normalization of energy with the energy in the solid at the interface. —, in the solid; ·····, in the fluid.

transducer (Panasonics, diameter 28 mm, resonance frequency 110 kHz). The wedge was made of Teflon<sup>®</sup>, a plastic material with weak shear wave velocity (measured velocity 550 m/s). The angle of the wedge was calculated to ensure the conversion of an incident shear wave into an interface wave at the water/solid material (PVC or B2900) interface:

$$\sin \theta = c_t \text{Teflon}^{\text{®}} / c_{sch}. \tag{24}$$

Its value was about 36° for PVC and 25° for B2900. The transmitter and the solid wedge were bonded by a coupling (SWC Sofranel), respectively to the Teflon<sup>®</sup> material and to the solid sample (PVC or B2900). The signals were received by a large bandwidth hydrophon (diameter 1 mm) situated in the water near the surface of the solid sample (distance less than 1 mm). The experiments took place in a tank of average dimensions

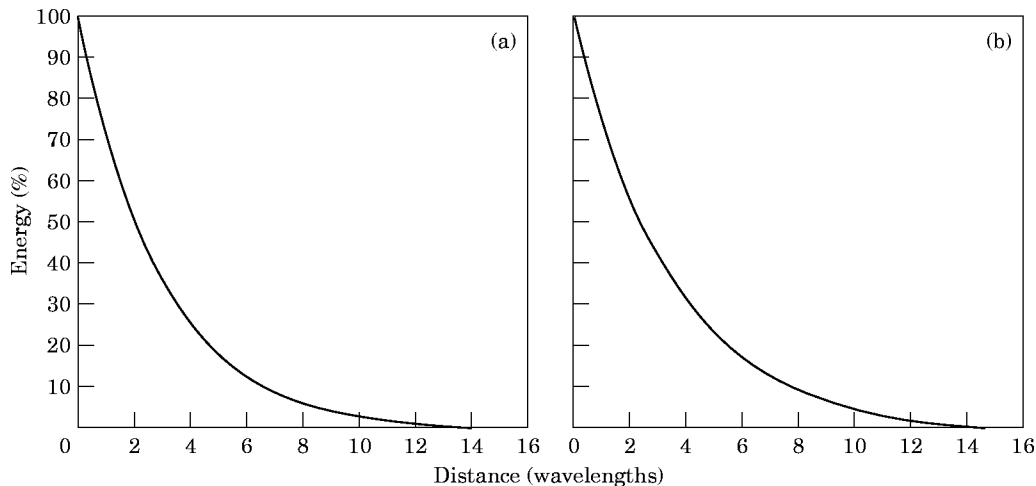


Figure 5. The theoretical attenuation of the energy of the Stoneley-Scholte wave during its propagation at the interface. (a) Water/PVC; (b) water/B2900. Frequency 60 kHz, wavelengths  $\lambda = 2.1$  cm for B2900 and  $\lambda = 1.5$  cm for PVC; normalization of energy with the energy near the source.

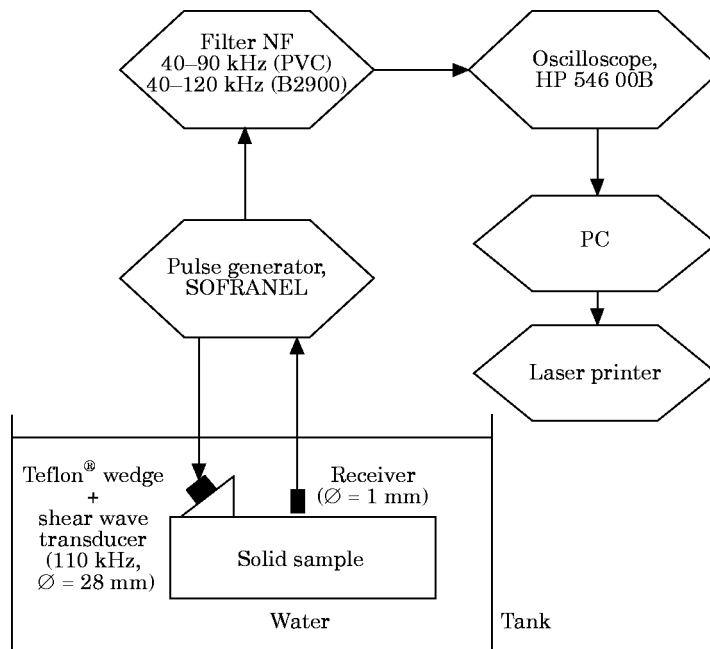


Figure 6. A schematic representation of the experimental set-up.

( $2.5 \times 1 \times 1 \text{ m}^3$ ) fitted out with stepping motors. The parallelepipedic samples were immersed in pure water to a depth 300 mm. The thicknesses of the samples (PVC, 83 mm; B2900, 78 mm) were large relative to the wavelengths of the Stoneley–Scholte wave ( $\lambda_{s \text{ PVC}} = 8 \text{ mm}$ ,  $\lambda_{s \text{ B2900}} = 1.2 \text{ cm}$  at the frequency 110 kHz). In both experiments, pulsed waves were produced by a pulse generator (Sofranel). The signals detected by the receiver were filtered (40–90 kHz for PVC and 40–120 kHz for B2900) and displayed on the screen of a numerical oscilloscope (HP 546 00 B). They were then recorded by means of a PC.

#### 4.2. DETECTION OF THE STONELEY–SCHOLTE WAVE

Typical waveforms and their spectra are represented in Figures 7 and 8. The emitter produces mainly shear waves, but it also produces compressional ones in reaction to the imposed shear strains. The Teflon® material is highly attenuating, in particular for the shear waves (measured attenuations:  $\alpha_t = 0.36 \text{ dB/m/kHz}$ ,  $\alpha_r = 2.5 \text{ dB/m/kHz}$ ). In Figures 9 and 10 are shown the spectra of the longitudinal and shear components of the emitter and those received after wave propagation into the 8 cm thick Teflon® material. It may therefore be concluded that the most significant signal detected near the surface of the solid sample (PVC or B2900) by the receiver corresponds to the Stoneley–Scholte wave excited by the shear component. The central frequency of its spectrum is about 70 kHz, which is different from the resonance frequency of the emitter. The first signal corresponds to a signal issued from the longitudinal component of the emitter. The central frequency of its spectrum is about 110 kHz.

These facts were entirely verified by measuring the velocity of the presumed Stoneley–Scholte wave. The measured value of the velocity  $c_0$  of sound in water was 1478 m/s. The experimental measurement of the velocity  $c_{sch}$  of the Stoneley–Scholte wave was on average  $866 \pm 10 \text{ m/s}$  for the water/PVC interface and  $1260 \pm 10 \text{ m/s}$  for the water/B2900 interface, which confirms the results predicted by the theory.

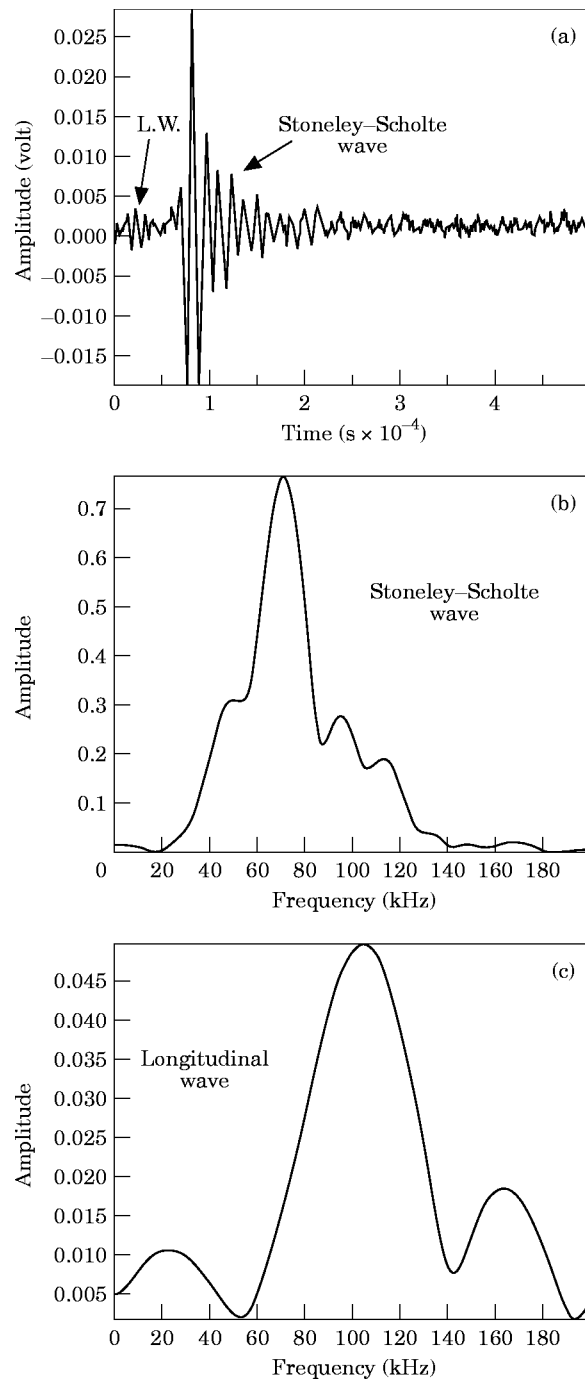


Figure 7. Signals detected by the receiver at the water/PVC interface (a) and their spectra (b) and (c). Wedge-receiver distance = 6 cm.

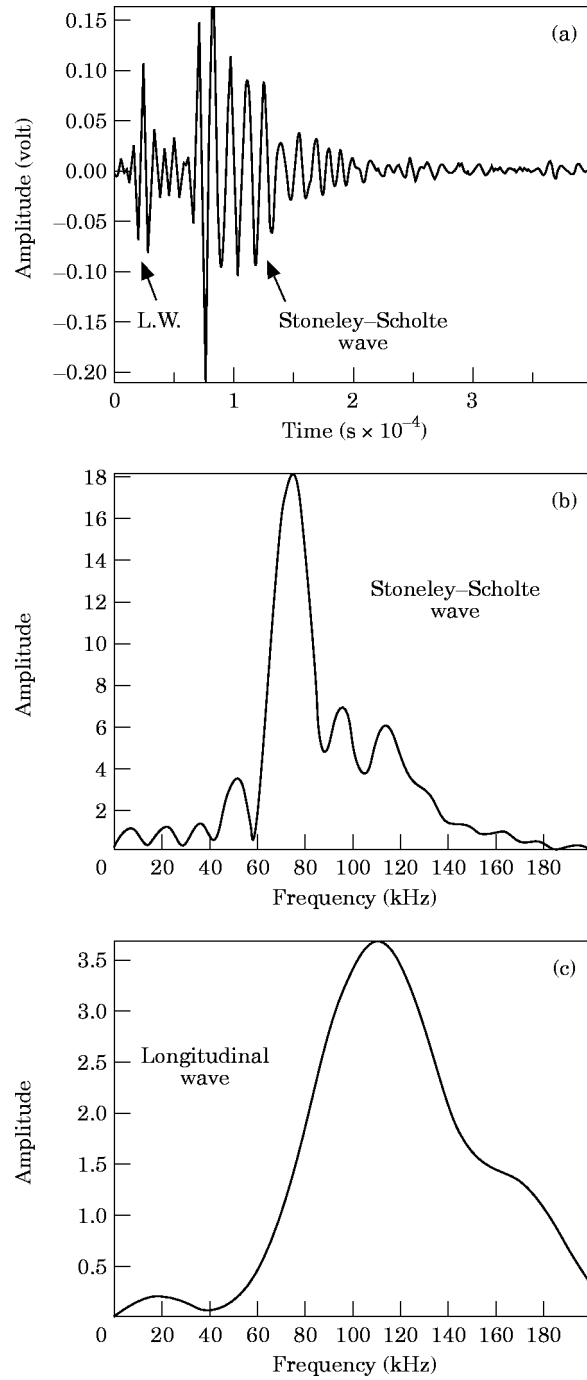


Figure 8. Signals detected by the receiver at the water/B2900 interface (a) and their spectra (b) and (c). Wedge-receiver distance = 3.8 cm.

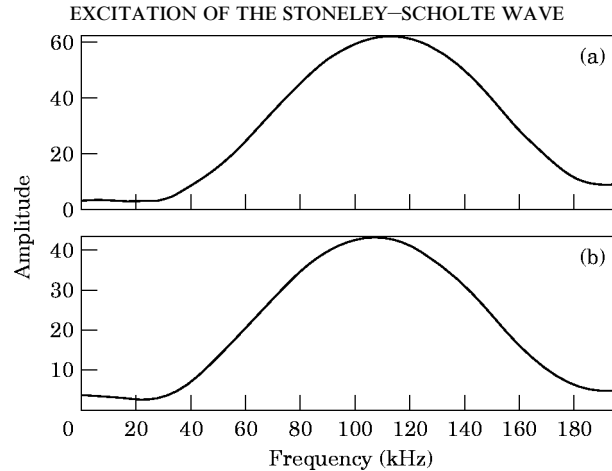


Figure 9. (a) The spectrum of the signal associated with the longitudinal waves produced by the emitter. (b) A numerical simulation of the spectrum associated with the longitudinal waves after propagation into 8 cm thick Teflon<sup>®</sup> material.

#### 4.3. DAMPING OF THE STONELEY–SCHOLTE WAVE RELATIVE TO DISTANCE FROM THE INTERFACE

The energy of the Stoneley–Scholte wave varies with the distance from the interface. This is illustrated by the curves in Figure 11 for the water/PVC interface and in Figure 12 for the water/B2900 one. On each figure, and for comparison, we have plotted the data deduced from the theory. The curves are normalized to the energy of the signal observed for the initial distance  $d_0$  from the wedge and for the initial distance  $d_1$  from the interface, defined subsequently.

The experiments were performed in the following conditions. For the water/PVC interface, the initial distance  $d_0$  between the receiver and the wedge was about 2 cm. The distance from the interface varied by moving the receiver, and measurements were carried out in the fluid every 0.1 mm from  $d_1 = 0.6$  mm to 1 mm, then every 0.2 mm from 1.2 mm

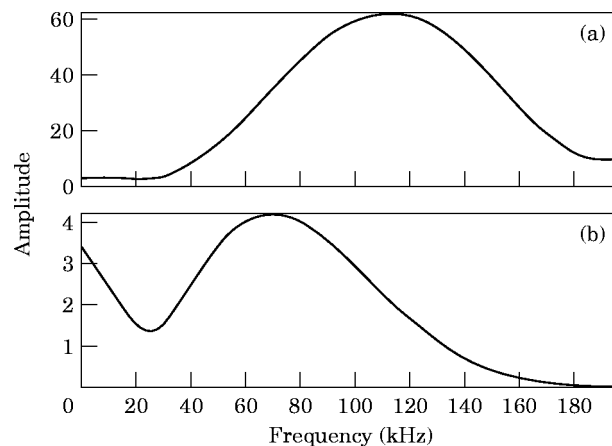


Figure 10. (a) The spectrum of the signal associated with the shear waves produced by the emitter. (b) A numerical simulation of the spectrum associated with the shear waves after propagation into 8 cm thick Teflon<sup>®</sup> material.

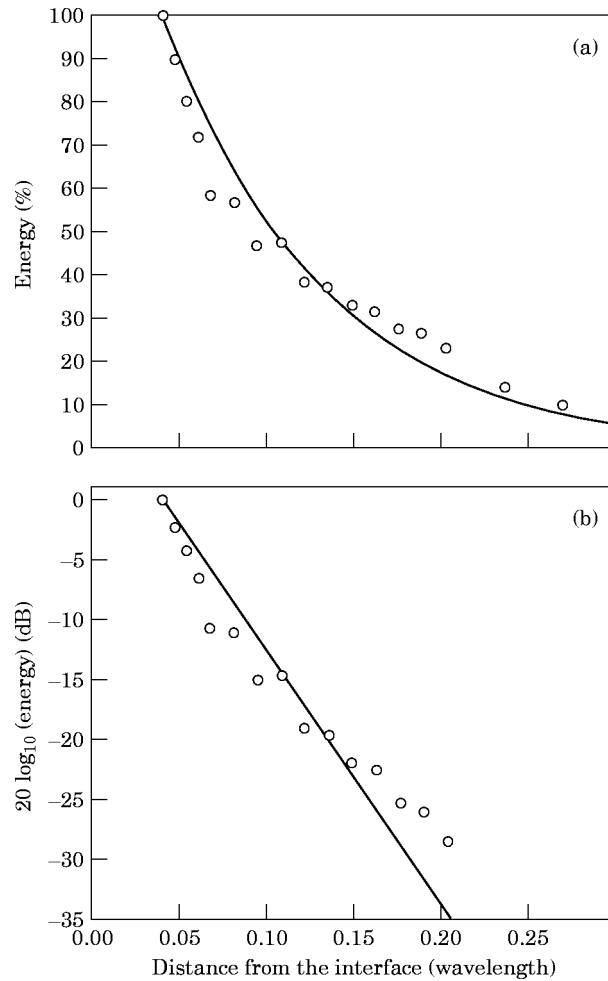


Figure 11. (a) A comparison between theoretical (—) and experimental (O) results: attenuation of the energy of the Stoneley-Scholte wave as a function of distance from the water/PVC interface. (b) Differences between theoretical (—) and experimental (O) results, quantified in dB. Frequency 60 kHz, wavelength  $\lambda=1.5$  cm; normalization of energy with the energy obtained for the first position of the receiver (0.6 mm from the interface and 2 cm from the source).

to 3 mm, and finally every 0.5 mm from 3.5 mm to 4 mm. For the water/B2900 interface, the initial distance  $d_0$  was about 3 cm. Measurements were taken in the fluid at every 0.2 mm, from  $d_1=0.4$  mm to 7.6 mm. The energies of the signals were recorded for each frequency. The experimental results for the water/PVC and for the water/B2900 interfaces, for example at 60 kHz and at 110 kHz, are shown in Figures 11 and 12.

For each experiment, the energy of the signal decreased exponentially with the distance from the interface, as predicted by theory. The agreement between the measured data and the theoretical prediction was good for every frequency. However, the experimental results did not correlate with the theoretical ones when the receiver was too far from the interface. Indeed, in this case, the signal:noise ratio decreases, and the energy of the signal corresponds almost entirely to that of the noise. The experimental and theoretical results also differed when the receiver was too close to the solid surface. Indeed, the solid sample

exerted a great stress on the transducer, and thus the energy of the signal was not normal. Therefore, recording of the energy started at the initial distance  $d_1$  from the interface.

4.4. DAMPING OF THE STONELEY-SCHOLTE WAVE DURING THE PROPAGATION AT THE INTERFACE

In Figures 13 and 14 are represented the variations of the energy of the Stoneley-Scholte wave along the water/PVC and the water/B2900 interfaces. The differences between the theoretical values and the experimental ones are also shown. The curves are normalized to the energy of the signal observed for the initial distance  $d_0$  from the wedge, defined subsequently.

The experiments were performed in the following conditions. For the water/PVC interface, the initial distance  $d_0$  between the receiver and the wedge was about 3 cm. Measurements were taken in the fluid very close to the solid sample (distance equal to  $\pm 0.5$  mm) every 5 mm from  $d_0$  to  $(d_0 + 16$  cm). For the water/B2900 interface, the initial

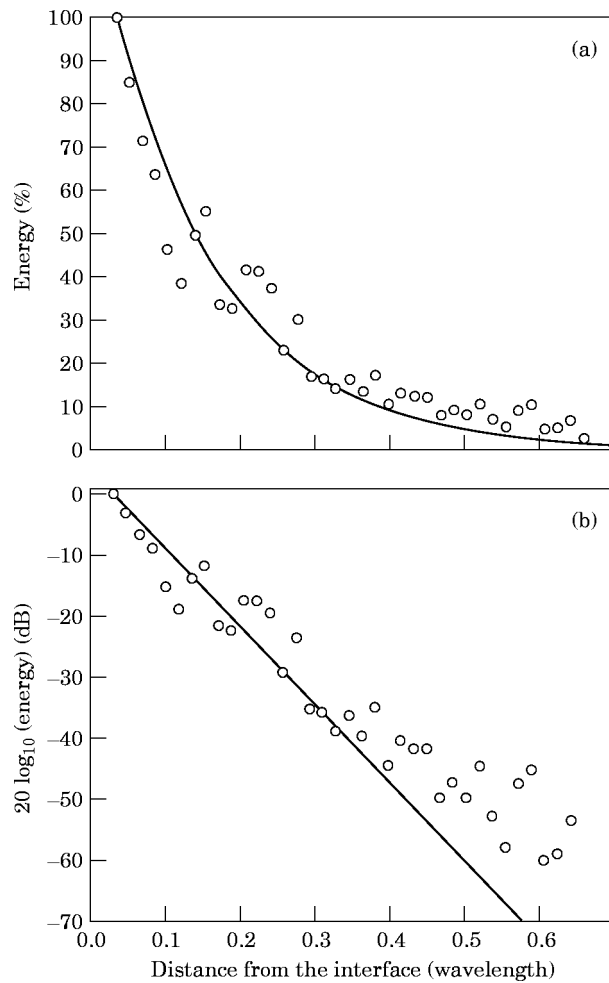


Figure 12. (a) A comparison between theoretical (—) and experimental (○) results: attenuation of the energy of the Stoneley-Scholte wave as a function of distance from the water/B2900 interface. (b) Differences between theoretical (—) and experimental (○) results, quantified in dB. Frequency 110 kHz, wavelength  $\lambda=1.2$  cm; normalization of energy with the energy obtained for the first position of the receiver (0.4 mm from the interface and 3 cm from the source).

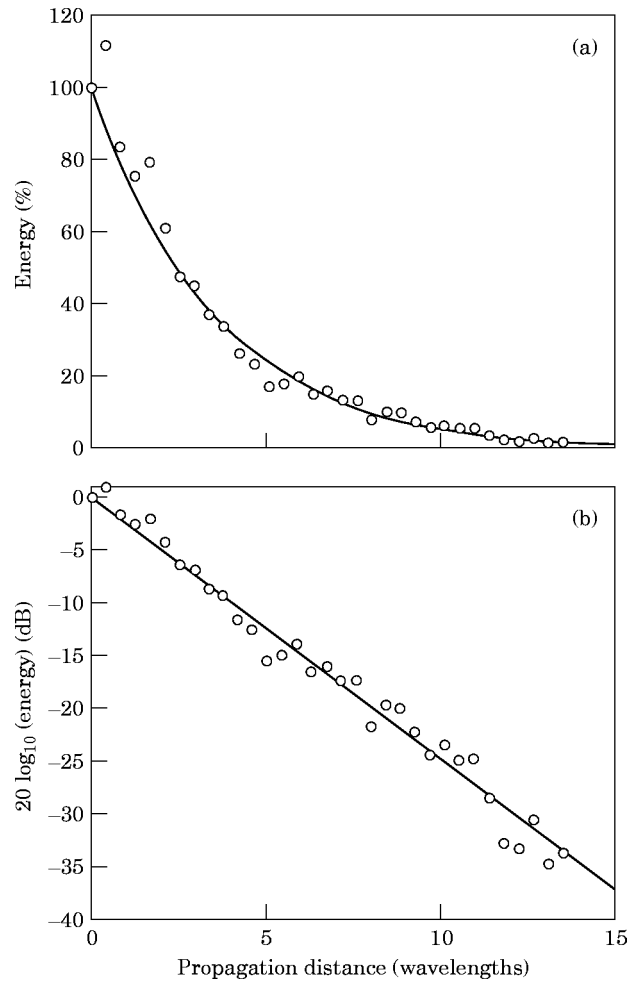


Figure 13. (a) A comparison between theoretical (—) and experimental (○) results: attenuation of the energy of the Stoneley–Scholte wave as a function of distance of propagation at the water/PVC interface. (b) Differences between theoretical (—) and experimental (○) results, quantified in dB. Frequency 75 kHz, wavelength  $\lambda = 1.2$  cm; normalization of energy with the energy obtained for the first position of the receiver (3 cm from the source).

distance  $d_0$  was about 3 cm. Measurements were taken in the fluid every 2 mm from  $d_0$  to  $(d_0 + 10$  cm), then every 5 mm from  $(d_0 + 10.5$  cm) to  $(d_0 + 20$  cm). The energies of the signals were recorded for each frequency. The experimental results for the water/PVC and for the water/B2900 interfaces, for example at 75 kHz and at 70 kHz, are shown in Figures 13 and 14.

For each frequency, the results of each experiment verified the rapidly decreasing energy of the wave during its propagation, as predicted by the theory. The Stoneley–Scholte wave was completely attenuated at the boundary between water and the solid sample at the end of a 15 cm propagation. This is due to the viscoelastic property of the solid material simulating the bottom.

In Figure 14(b), the difference between the theoretical and the estimated values of the energy is about 2.5 dB. In fact, there is always some inaccuracy about the absolute distance

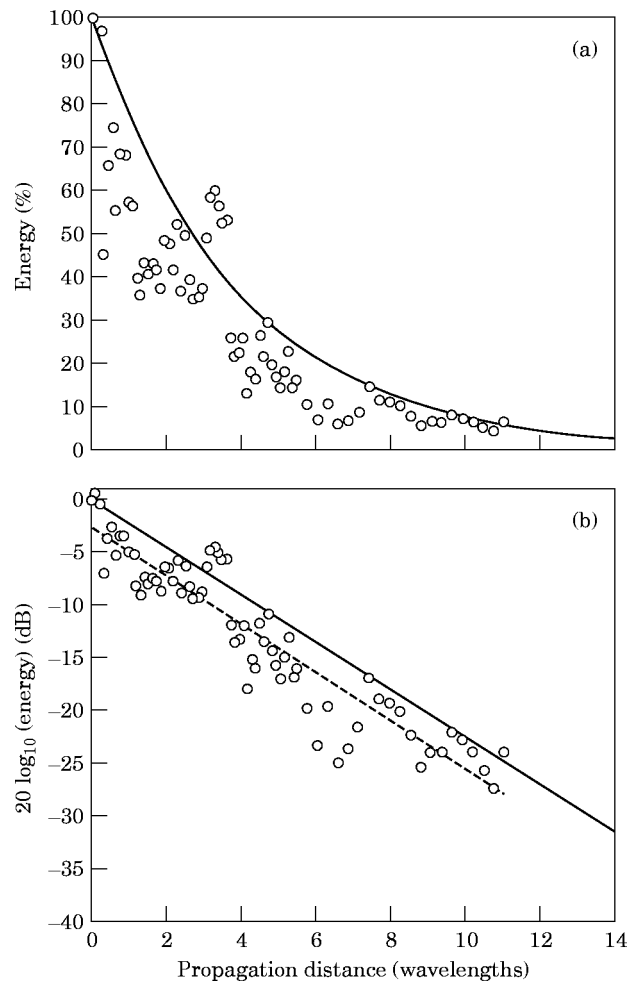


Figure 14. (a) A comparison between theoretical (—) and experimental (○) results: attenuation of the energy of the Stoneley-Scholte wave as a function of distance of propagation at the water/B2900 interface. (b) Differences between theoretical (—) and experimental (○) results, quantified in dB. - - -, The slope obtained by the least squares fit of the experimental data. Frequency 70 kHz, wavelength  $\lambda = 1.8$  cm; normalization of energy with the energy obtained for the first position of the receiver (3 cm from the source).

from the receiver to the solid material; the position of the receiver is accurate only within 0.2 mm. This implies a decrease in the energy of 2.5 dB, as is shown in Figure 12.

## 5. CONCLUSIONS

The Stoneley-Scholte wave has been generated at a plane water/viscoelastic solid interface by using a solid wedge and a shear wave transducer. The viscoelastic solid was represented by PVC material and also by a synthetic resin (B2900). Thus, it has been quantitatively verified that the Stoneley-Scholte wave is attenuated as a function of distance from the interface. However, above all, the experiment has confirmed the damping of the propagation of the interface wave at the boundary between water and a viscoelastic solid, with a slower speed than that of the homogeneous plane waves in media. These

findings thus prove the validity of the previous study [5] of the Stoneley–Scholte wave at the plane boundary between an ideal fluid and a viscoelastic solid.

Thanks to the experimental and theoretical studies of the propagation of the Stoneley–Scholte wave, the authors expect soon to be able to determine the shear wave parameters of the viscoelastic solid by using an inverse method (conjugate gradients, etc.). The final topic of this continuing investigation is the characterization of the shear wave velocity and attenuation of a sedimentary bottom, simulated in the work by a viscoelastic solid, by means of the dispersion curves and the density of the energy of the interface waves.

#### ACKNOWLEDGMENTS

The authors would like to thank Dr J.-P. Sessarego for his advice, J.-Y. Jaskulski for his help with this experimental study and G Burkhart for his help with the English translation.

#### REFERENCES

1. B. POIRÉE and F. LUPPÉ 1991 *Journal d'Acoustique* **4**, 575–588. Evanescent plane waves and the Scholte–Stoneley interface waves.
2. F. B. JENSEN and H. SCHMIDT 1986 in *Ocean Seismo-acoustics* (T. Akal and J. M. Berkson, editors), 683–692. New York: Plenum Press. Shear properties of ocean sediments determined from numerical modelling of Scholte wave data.
3. A. CAITI, T. AKAL and R. D. STOLL 1991 in *Shear Waves in Marine Sediments* (J. M. Hovem, M. D. Richardson and R. D. Stoll, editors), 557–566. Dordrecht: Kluwer Academic. Determination of shear velocity profiles by inversion of interface wave data.
4. M. M. VOL'KENShteIN and V. M. LEVIN 1988 *Soviet Physics—Acoustics* **34**(4), 351–355. Structure of a Stoneley wave at an interface between a viscous fluid and a solid.
5. N. FAVRETTO-ANRÈS 1996 *Acustica united with Acta Acustica* **82**(6), 829–838. Theoretical study of the Stoneley–Scholte wave at the interface between an ideal fluid and a viscoelastic solid.
6. F. LUPPÉ and J. DOUCET 1988 *Journal of the Acoustical Society of America* **83**(4), 1276–1280. Experimental study of the Stoneley wave at a plane liquid/solid interface.
7. M. DE BILLY and G. QUENTIN 1983 *Journal of Applied Physics* **54**(8), 4314–4322. Experimental study of the Scholte wave propagation on a plane surface partially immersed in a liquid.
8. J.-M. CLAEYS, O. LEROY, A. JUNGMAN and L. ADLER 1983 *Journal of Applied Physics* **54**(10), 5657–5662. Diffraction of ultrasonic waves from periodically rough liquid/solid surface.
9. S. N. GUZHEV, V. M. LEVIN, R. G. MAEV and M. KOTELIJANSKII 1984 *Soviet Physical and Technical Physics* **29**, 817–818. Excitation of Stoneley surface acoustic waves at a solid/liquid interface using an interdigitated transducer.
10. I. A. VIKTOROV 1967 *Rayleigh and Lamb Waves* (W. P. Mason, editor), New York: Plenum Press.
11. J. GUILBOT 1994 *Ph.D. Thesis, INSA de Lyon*. Caractérisation acoustique de fonds sédimentaires marins par étude de la dispersion de célérité des ondes d'interface de type Stoneley–Scholte.
12. B. POIRÉE 1989 *Journal d'Acoustique* **2**, 205–216. Les ondes planes évanescences dans les fluides et les solides élastiques.
13. B. POIRÉE 1991 in *Physical Acoustics* (O. Leroy and M. A. Breazeale, editors), New York: Plenum Press, 99–117. Complex harmonic plane waves.
14. M. DESCHAMPS 1991 *Journal d'Acoustique* **4**, 269–305. L'onde plane hétérogène et ses applications en acoustique linéaire.